

## ***Supporting Information***

### **Catalyst-free synthesis of diverse fluorescent polyoxadiazoles for the facile formation and morphology visualization of microporous films and cell imaging**

Junyao Xie,<sup>†</sup> Niu Niu,<sup>†, ‡</sup> Xinyao Fu,<sup>§</sup> Xiang Su,<sup>†</sup> Dong Wang,<sup>†</sup> Anjun Qin,<sup>§</sup> Ting Han,<sup>\*, †</sup> and Ben Zhong Tang<sup>\*, †</sup>

<sup>†</sup>Center for AIE Research, Shenzhen Key Laboratory of Polymer Science and Technology, Guangdong Research Center for Interfacial Engineering of Functional Materials, College of Materials Science and Engineering, Shenzhen University, Shenzhen 518060, China

<sup>‡</sup>College of Physics and Optoelectronic Engineering, Shenzhen University, Shenzhen 518060, China

<sup>§</sup>State Key Laboratory of Luminescent Materials and Devices, Guangdong Provincial Key Laboratory of Luminescence from Molecular Aggregates, Center for Aggregation-Induced Emission, AIE Institute, South China University of Technology, Guangzhou 510640, China

<sup>||</sup>School of Science and Engineering, Shenzhen Institute of Aggregate Science and Technology, The Chinese University of Hong Kong, Shenzhen, Guangdong 518172, China

## Table of Contents

<b>Experimental Section</b> .....	4
<b>Scheme S1.</b> Possible mechanism for the formation of 2,5-disubstituted 1,3,4-oxadiazole derivatives. ...	9
<b>Table S1.</b> Optimization of the polymerization conditions for the synthesis of hyperbranched polymers.	9
<b>Scheme S2.</b> Synthetic route to model compound <b>5</b> . .....	10
<b>Figure S1.</b> IR spectra of (A) <b>1a</b> , (B) <b>2a</b> , (C) <b>3a</b> , (D) <b>4</b> , (E) model compound <b>5</b> , and (F) <b>P1</b> . .....	10
<b>Figure S2.</b> IR spectra of (A) <b>P2</b> , (B) <b>P3</b> , (C) <b>P4</b> , (D) <b>P5</b> , (E) <b>P6</b> . .....	11
<b>Figure S3.</b> IR spectra of (A) <i>hb-P1</i> , (B) <i>hb-P2</i> , and (C) <i>hb-P3</i> . .....	11
<b>Figure S4.</b> <sup>1</sup> H NMR spectra of (A) <b>P2</b> , (B) <b>P3</b> , (C) <b>P4</b> , (D) <b>P5</b> , and (E) <b>P6</b> in DMSO- <i>d</i> <sub>6</sub> . .....	12
<b>Figure S5.</b> <sup>1</sup> H NMR spectra of (A) <i>hb-P1</i> , (B) <i>hb-P2</i> , (C) <i>hb-P3</i> in DMSO- <i>d</i> <sub>6</sub> . .....	13
<b>Figure S6.</b> <sup>13</sup> C NMR spectra of (A) <b>P2</b> , (B) <b>P3</b> , (C) <b>P4</b> , (D) <b>P5</b> , and (E) <b>P6</b> in DMSO- <i>d</i> <sub>6</sub> . .....	14
<b>Figure S7.</b> <sup>13</sup> C NMR spectra of (A) <i>hb-P1</i> , (B) <i>hb-P2</i> , and (C) <i>hb-P3</i> in DMSO- <i>d</i> <sub>6</sub> . .....	15
<b>Figure S8.</b> TGA thermograms of (A) linear polymers <b>P1–P6</b> and (B) hyperbranched polymers <i>hb-P1–hb-P3</i> recorded under nitrogen at a heating rate of 10 °C/min. ....	16
<b>Figure S9.</b> DSC thermograms of (A) <b>P1–P6</b> and (B) <i>hb-P1–hb-P3</i> recorded under nitrogen during the second heating cycle at a heating rate of 10 °C/min. ....	17
<b>Figure S10.</b> UV-vis absorption spectra and the maximum absorption wavelengths of <b>P1–P6</b> and <i>hb-P1–hb-P3</i> in their THF solutions. Solution concentration: 10 μM. ....	17
<b>Table S2.</b> Fluorescence quantum yields of polymers in different states. ....	17
<b>Figure S11.</b> Normalized UV-vis absorption spectra of <i>hb-P1</i> and <i>hb-P2</i> in different states and the normalized PL spectrum of TPE in THF solution. Solution concentration: 10 μM. The absorption spectra of <i>hb-P1</i> and <i>hb-P2</i> aggregates were measured on their THF/water suspension with a water fraction of 90%. ....	18
<b>Figure S12.</b> (A) SEM and (B) TEM images of the thin films prepared by the solvent evaporation of the chloroform solution of polymer <b>P3</b> on the surface of a silicon wafer or TEM support grids. Solution concentration: 0.01 mg/mL. ....	18
<b>Figure S13.</b> Fluorescence image showing the morphology of the thin film obtained by the solvent evaporation of the chloroform solution of <b>P6</b> on a silicon wafer. Solution concentration: 0.1 mg/mL... ..	19
<b>Figure S14.</b> Experimental set-up for the fabrication of porous thin films of <b>P6</b> using the breath figure method. ....	19

**Figure S15.** (A–C) SEM images of the film morphology formed by the chloroform solution of P6 (1.0 mg/mL) using different methods of establishing humid environment. (D–F) SEM images showing the influence of organic solvents on the film morphology of P6. Solution concentration: 1.0 mg/mL. (G–I) SEM images showing the influence of the concentration of the chloroform solution of P6 on the film morphology. .... 20

**Figure S16.** (A) The bright-field image, (B) fluorescence image, and (C) the merged image of the fluorescence images and the bright-field image of 4T1 cells stained with P6 (10 µg/mL, 2 h). Scale bar = 10 µm. Excitation wavelength: 405 nm; emission filter: 420–650 nm..... 20

**Figure S17.** (A and B) Confocal images of 4T1 cells stained with (A) P6 (20 µg/mL, 4 h, DMSO stock solution) and (B) LysoTracker Red (LTR, 1 µM, 30 min). (C) The associated bright-field image. (D) The merged image of the fluorescence images and the bright-field image. Scale bar = 10 µm. Excitation wavelength: 405 nm for polymers and 561 nm for LTR; emission filter: 420–650 nm for polymers and 650–700 nm for LTR..... 21

**Figure S18.** Cell viability of 4T1 cells in the presence of P6 (DMSO stock solution) at different concentrations..... 21

**Figure S19.** Cell viability of 4T1 cells in the presence of *hb*-P3 (DMSO stock solution) at different concentrations..... 22

**Figure S20.** Fluorescence images of 4T1 cells obtained at different scan time. The 4T1 cells were stained with (A) P6 nanoparticles (20 µg/mL, 4 h) and (B) *hb*-P3 nanoparticles (20 µg/mL, 4 h).... 22

**References** ..... 22

## Experimental Section

### Materials and Instrumentation

Terephthalaldehyde (**1a**), terephthalic acid (**2a**), dibenzylamine (**3a**), (*N*-isocyanimino)triphenylphosphorane **4**, and all other chemicals and reagents were purchased from commercial suppliers including Bidepharm, Meryer, Aladdin, Energy and Adamas, and they were used as received without further purification. Solvents such as dichloromethane (DCM), *N,N*-Dimethylformamide (DMF), dimethylacetamide (DMAc) Methanol (MeOH) and tetrahydrofuran (THF) were ultra-dry reagents with molecular sieves and were purchased from J&K Scientific. The aromatic dicarboxylic acids **2b** and **2c** were purchased from D&B and Kaimuke. Aromatic dialdehydes **1c** and **1d**, triphenylamine (TPA)-containing tricarboxylic acid (**2d**), and TPE-containing tetracarboxylic acid (**2e**) were prepared according to the previously reported procedures.<sup>[1]</sup> Phosphate buffered saline (PBS), fetal bovine serum (FBS) and Roswell Park Memorial Institute (RMPI-1640) medium were purchased from Gibco. LysoTracker Red and 3-(4,5-dimethylthiazol-2-yl)-2,5-diphenyltetrazolium bromide (MTT) was purchased from Invitrogen and Molecular Probes, respectively, in Thermo Fisher Scientific.

<sup>1</sup>H and <sup>13</sup>C NMR spectra were estimated on a Bruker AVANCE III 600 or 500 MHz NMR spectrometer at 298 K. Chemical shifts were calibrated using DMSO-*d*<sub>6</sub> (<sup>1</sup>H NMR:  $\delta$  2.50 ppm; <sup>13</sup>C NMR:  $\delta$  39.52 ppm) as internal reference. FT-IR spectra were determined on a Nicolet 6700 FTIR spectrophotometer. Absolute molecular weights were obtained by tandem GPC experiments using a system equipped with an isocratic pump (Waters e2695), a DAWN HELESO II multi-angle laser light scattering (MALLS) detector and an Optilab rEX refractive index detector (Wyatt technology, Santa Barbara, CA). The separations were carried out using size-exclusion columns connected in series at 40 °C with THF as the mobile phase. The absolute *M*<sub>w</sub> of polymers were calculated by their refractive index increment (dn/dc) values that were determined offline using the internal calibration system (ASTRA software, version 7.3.2, Wyatt Technology, Santa Barbara, CA). Thermogravimetric analysis (TGA) and differential scanning calorimetry (DSC) measurement was carried out on a TA TGA 55 and a TA DSC Q200, respectively, under nitrogen at a heating rate of 10 °C/min. UV-vis spectra and photoluminescence (PL) spectra were measured on a Shimadzu UV-2450 UV/Vis spectrophotometer and an Edinburgh FS5 fluorescence spectrometer, respectively. A high-resolution scanning electron microscope (HRSEM, Thermo APREO S) was used for examination of the surface morphology after specimen sputtering with gold using Automatic ion sputtering instrument. Transmission electron microscope (TEM) images were recorded on a JEOL-F200 TEM, and the samples were prepared by dropping polymer solutions onto carbon supported copper grids. The absolute PL quantum yields were determined by a Quantaaurus-QY absolute PL quantum yield spectrometer (Hamamatsu C11347). The fluorescence images of breath figures were taken by an inverted fluorescence microscope (Olympus IX73).

### Synthesis and Characterization

#### Model reaction:

The synthetic procedures of model compound **5** were provided as follows. To a magnetically stirred solution of dibenzylamine (192  $\mu$ L, 1 mmol), benzaldehyde (106 mg, 1 mmol) and (*N*-isocyanimino)triphenylphosphorane (302 mg, 1 mmol) in CH<sub>2</sub>Cl<sub>2</sub> (5 mL) was added dropwise of a

solution of benzoic acid (122 mg, 1 mmol) in CH<sub>2</sub>Cl<sub>2</sub> (5 mL) at room temperature over 15 min. The reaction mixture was stirred at room temperature for 12 h. After solvent removal, the residue was purified by silica gel flash column chromatography (eluent: petroleum ether/ethyl acetate = 2/1, v/v) to give the desired product **5** as a colorless oil (yield 86%). IR (neat),  $\nu$  (cm<sup>-1</sup>): 3059, 3025, 2915, 2822, 1608, 1585, 1551, 1491, 1450, 1368, 1246, 1117, 1069, 1009, 961, 910, 841, 743, 695, 495. <sup>1</sup>H NMR (500 MHz, DMSO-*d*<sub>6</sub>)  $\delta$  8.02–7.99 (m, 2H), 7.69–7.60 (m, 3H), 7.50–7.32 (m, 13H), 7.23 (tt, *J* = 7.3, 1.3 Hz, 2H), 5.33 (s, 1H), 3.75 (d, *J* = 10.0 Hz, 2H), 3.63 (d, *J* = 15 Hz, 2H) <sup>13</sup>C NMR (125 MHz, DMSO-*d*<sub>6</sub>)  $\delta$  164.52, 164.30, 138.51, 136.22, 131.90, 129.27, 128.60, 128.35, 128.15, 127.12, 126.62, 123.32, 59.18, 53.94. Model compound **5** was synthesized according to reported procedures.<sup>[21]</sup>

### Synthesis of Linear Polymers:

The synthetic procedure to **P1** (Table 1, entry 2) was given below as an example. To an oven-dried 4-mL vial equipped with a magnetic stir were sequentially added terephthalaldehyde **1a** (27 mg, 0.2 mmol), terephthalic **2a** (33 mg, 0.2 mmol), (*N*-isocyanimino)triphenylphosphorane **4** (145 mg, 0.48 mmol), DMSO (2 mL), and dibenzylamine **3a** (92  $\mu$ L, 0.48 mmol) under N<sub>2</sub> atmosphere in a glove box. The reaction mixture was then stirred outside the glovebox at room temperature for 24 h. Upon completion, the resulting solution was diluted with 3 mL of THF and then added dropwise into 150 mL of MeOH. The precipitate was finally collected after filtration, being washed with MeOH, and dried under vacuum at 50 °C to a constant weight. The structural characterization results were summarized as follows.

*Characterization Data for P1:* yellowish-white powder. 74% yield; *M*<sub>n</sub>: 24800; *M*<sub>w</sub>: 37100; *M*<sub>w</sub>/*M*<sub>n</sub>: 1.5 (MALLS). IR (neat),  $\nu$  (cm<sup>-1</sup>): 3059, 3025, 2892, 2833, 1685, 1599, 1584, 1548, 1491, 1448, 1414, 1366, 1245, 1108, 1071, 1010, 963, 909, 850, 744, 695, 532. <sup>1</sup>H NMR (500 MHz, DMSO-*d*<sub>6</sub>)  $\delta$  (ppm): 8.13 (aromatic protons), 7.66–6.81 (aromatic protons), 5.36 (CH protons), 3.70–3.61 (NCH<sub>2</sub> protons). <sup>13</sup>C NMR (125 MHz, DMSO-*d*<sub>6</sub>)  $\delta$  (ppm): 164.77, 163.89, 138.49, 136.27, 132.71, 126.74, 126.03, 59.10, 54.05.

*Characterization Data for P2:* white powder. 58% yield; *M*<sub>n</sub>: 15800; *M*<sub>w</sub>: 31400; *M*<sub>w</sub>/*M*<sub>n</sub>: 2.0 (MALLS). IR (neat),  $\nu$  (cm<sup>-1</sup>): 3059, 3025, 2935, 2839, 1704, 1601, 1581, 1544, 1492, 1452, 1414, 1366, 1249, 1122, 1074, 1026, 1006, 961, 910, 850, 742, 695, 532. <sup>1</sup>H NMR (500 MHz, DMSO-*d*<sub>6</sub>)  $\delta$  (ppm): 8.33–8.09 (aromatic protons), 7.46–7.00 (aromatic protons), 4.05–3.75 (CH and NCH<sub>2</sub> protons), 2.10, 1.86, 1.61. <sup>13</sup>C NMR (125 MHz, DMSO-*d*<sub>6</sub>)  $\delta$  (ppm): 165.73, 163.36, 138.84, 128.61, 128.61, 128.27, 127.56, 127.07, 126.68, 126.80, 126.30, 126.10, 53.57.

*Characterization Data for P3:* brownish yellow powder. 22% yield; *M*<sub>n</sub>: 37700; *M*<sub>w</sub>: 83800; *M*<sub>w</sub>/*M*<sub>n</sub>: 2.2 (MALLS). IR (neat),  $\nu$  (cm<sup>-1</sup>): 3058, 3029, 2972, 2835, 1699, 1585, 1552, 1489, 1452, 1417, 1376, 1261, 1202, 1165, 1059, 1008, 960, 911, 853, 793, 704, 526. <sup>1</sup>H NMR (500 MHz, DMSO-*d*<sub>6</sub>)  $\delta$  (ppm): 8.07 (aromatic protons), 7.49 (aromatic protons), 5.48 (CH protons), 2.61 (NCH<sub>2</sub> protons), 0.94 (CH<sub>3</sub> protons). <sup>13</sup>C NMR (125 MHz, DMSO-*d*<sub>6</sub>)  $\delta$  (ppm): 166.45, 164.19, 137.51, 131.99, 131.92, 130.11, 129.28, 129.18, 128.78, 128.04, 127.36, 126.46, 66.67, 60.61, 44.05, 40.90, 12.96.

*Characterization Data for P4:* yellow powder. 57% yield; *M*<sub>n</sub>: 11600; *M*<sub>w</sub>: 21500; *M*<sub>w</sub>/*M*<sub>n</sub>: 1.9 (MALLS). IR (neat),  $\nu$  (cm<sup>-1</sup>): 3062, 3029, 2926, 2827, 1706, 1585, 1545, 1491, 1450, 1415, 1367, 1257, 1205, 1114, 1074, 1004, 961, 910, 850, 738, 696, 527. <sup>1</sup>H NMR (500 MHz, DMSO-*d*<sub>6</sub>)  $\delta$  (ppm): 8.05 (aromatic protons), 7.60–7.35 (aromatic protons), 5.13 (CH protons), 2.35 (NCH<sub>2</sub> protons), 1.50–1.16 (CH<sub>2</sub> protons). <sup>13</sup>C NMR (125 MHz, DMSO-*d*<sub>6</sub>)  $\delta$  (ppm): 163.54, 160.20, 131.81, 131.42, 131.37, 131.31, 128.73, 128.64, 128.52, 127.43, 64.54, 51.10, 25.47, 23.69.

*Characterization Data for P5*: brownish-yellow powder. 64% yield;  $M_n$ : 13100;  $M_w$ : 22000;  $M_w/M_n$ : 1.7 (MALLS). IR (neat),  $\nu$  ( $\text{cm}^{-1}$ ): 3057, 3029, 2931, 2860, 1684, 1605, 1495, 1453, 1425, 1371, 1305, 1245, 1165, 1108, 1071, 1005, 961, 911, 832, 741, 695, 526.  $^1\text{H}$  NMR (500 MHz,  $\text{DMSO-}d_6$ ),  $\delta$  (ppm): 7.91–6.73 (aromatic protons), 5.21 (CH protons), 4.04–3.85 ( $\text{CH}_2$  protons), 3.69 ( $\text{CH}_2$  protons), 3.60 ( $\text{CH}_2$  protons), 1.82 ( $\text{CH}_2$  protons), 1.47 ( $\text{CH}_2$  protons).  $^{13}\text{C}$  NMR (125 MHz,  $\text{DMSO-}d_6$ ),  $\delta$  (ppm): 167.52, 164.81, 164.53, 161.94, 158.93, 139.13, 132.26, 131.78, 129.94, 128.83, 128.83, 128.37, 127.60, 115.97, 115.71, 115.34, 114.95, 114.76, 114.61, 68.42, 68.24, 67.81, 66.50, 59.06, 54.33, 29.03, 28.91, 25.71, 25.66.

*Characterization Data for P6*: white powder. 61% yield;  $M_n$ : 6800;  $M_w$ : 10200;  $M_w/M_n$ : 1.5 (MALLS). IR (neat),  $\nu$  ( $\text{cm}^{-1}$ ): 3054, 3026, 2931, 2848, 1683, 1606, 1546, 1495, 1445, 1365, 1306, 1248, 1170, 1113, 1075, 1025, 1004, 962, 912, 820, 743, 696, 527, 443.  $^1\text{H}$  NMR (500 MHz,  $\text{DMSO-}d_6$ ),  $\delta$  (ppm): 7.93–6.90 (aromatic protons), 5.31 (CH protons), 4.11–3.54 ( $\text{CH}_2$  protons), 1.75 ( $\text{CH}_2$  protons), 1.48 ( $\text{CH}_2$  protons).  $^{13}\text{C}$  NMR (125 MHz,  $\text{DMSO-}d_6$ ),  $\delta$  (ppm): 167.12, 164.47, 163.69, 161.51, 143.13, 142.43, 141.00, 139.50, 139.10, 138.53, 137.16, 135.45, 132.03, 131.86, 131.39, 131.28, 131.28, 130.52, 129.10, 128.79, 128.70, 128.51, 128.40, 128.28, 127.89, 127.19, 126.94, 126.86, 126.48, 125.80, 67.65, 58.91, 53.96, 28.46, 25.20.

### Synthesis of Hyperbranched Polymers:

The synthetic procedure to *hb-P3* (Figure 2B) was given below as an example. To an oven-dried 4-mL vial equipped with a magnetic stir were sequentially added terephthalaldehyde **1a** (27 mg, 0.1 mmol), **2e** (162 mg, 0.2 mmol), (*N*-isocyanimino)triphenylphosphorane **4** (145 mg, 0.48 mmol), DMSO (2 mL), and dibenzylamine **3a** (92  $\mu\text{L}$ , 0.48 mmol) under  $\text{N}_2$  atmosphere in a glove box. The reaction mixture was then stirred outside the glovebox at room temperature for 24 h. Upon completion, the resulting solution was diluted with 3 mL of THF and then added dropwise into 150 mL of MeOH. The precipitate was finally collected after filtration, being washed with MeOH, and dried under vacuum at 50  $^\circ\text{C}$  to a constant weight. The structural characterization results were summarized as follows.

*Characterization Data for hb-P1*: yellow powder. 50% yield;  $M_n$ : 6300;  $M_w$ : 9100;  $M_w/M_n$ : 1.4 (MALLS). IR (neat),  $\nu$  ( $\text{cm}^{-1}$ ): 3053, 3027, 2827, 1696, 1596, 1519, 1487, 1447, 1378, 1320, 1273, 1182, 1113, 1072, 1005, 961, 824, 736, 696, 534, 452.  $^1\text{H}$  NMR (600 MHz,  $\text{DMSO-}d_6$ ),  $\delta$  (ppm): 8.23–6.90 (aromatic protons), 5.36 (CH protons), 3.74–3.64 ( $\text{NCH}_2$  protons).  $^{13}\text{C}$  NMR (150 MHz,  $\text{DMSO-}d_6$ ),  $\delta$  (ppm): 167.04, 164.33, 147.01, 145.95, 138.32, 133.79, 133.13, 132.31, 132.05, 131.52, 131.45, 129.97, 128.80, 128.71, 128.39, 128.18, 128.06, 126.93, 126.68, 126.14, 124.32, 54.00, 51.96.

*Characterization Data for hb-P2*: yellow powder. 50% yield;  $M_n$ : 7600;  $M_w$ : 10800;  $M_w/M_n$ : 1.3 (MALLS). IR (neat),  $\nu$  ( $\text{cm}^{-1}$ ): 3057, 3027, 2910, 2828, 1696, 1597, 1519, 1488, 1447, 1378, 1323, 1275, 1185, 1112, 1074, 1003, 961, 822, 738, 694, 535, 453.  $^1\text{H}$  NMR (600 MHz,  $\text{DMSO-}d_6$ ),  $\delta$  (ppm): 8.15–6.89 (aromatic protons), 5.36 (CH protons), 3.75–3.65 ( $\text{NCH}_2$  protons).  $^{13}\text{C}$  NMR (150 MHz,  $\text{DMSO-}d_6$ ),  $\delta$  (ppm): 167.74, 164.96, 147.21, 143.63, 139.01, 134.21, 133.61, 132.49, 132.00, 131.92, 131.14, 130.46, 129.27, 129.18, 128.90, 128.65, 128.37, 127.44, 127.11, 127.11, 126.68, 126.40, 124.81, 59.42, 54.44.

*Characterization Data for hb-P3*: yellow powder. 49% yield;  $M_n$ : 8100;  $M_w$ : 12200;  $M_w/M_n$ : 1.5 (MALLS). IR (neat),  $\nu$  ( $\text{cm}^{-1}$ ): 3058, 3030, 2922, 2828, 1698, 1597, 1520, 1487, 1445, 1373, 1319, 1274, 1183, 1113, 1076, 1006, 963, 822, 738, 695, 532, 458.  $^1\text{H}$  NMR (600 MHz,  $\text{DMSO-}d_6$ ),  $\delta$  (ppm): 8.0–6.84 (aromatic protons), 5.31 (CH protons), 3.70–3.60 ( $\text{NCH}_2$  protons).  $^{13}\text{C}$  NMR (150 MHz,  $\text{DMSO-}d_6$ ),  $\delta$  (ppm): 167.67, 164.46, 143.63, 140.68, 138.96, 137.59, 133.57, 132.76, 132.51, 131.95, 130.38, 129.28, 129.19, 128.85, 128.64, 127.68, 126.91, 67.49, 54.52, 52.29.

### **Preparation and Characterization of Porous Thin Films by the Static Breath Figure Process:**

The experimental set-up for the preparation of porous thin films of P6 by static breath figure method was depicted in Figure S14. Typical preparation procedures are provided as follows. First, 1 mg of the solid powder of P6 was completely dissolved in 1 mL of chloroform under sonication to afford polymer solution with a concentration of 1.0 mg/mL. Next, to a clean glass petri dish was added into a certain amount of deionized water at room temperature. Meanwhile, a bottom support was placed in the glass petri dish and the surface of this bottom support was around 5 mm higher than the liquid level of deionized water. After a clean silicon wafer was placed on the bottom support, the whole device was sealed with plastic wrap and placed at room temperature for 30 min. Then the sealed device was heated at around 70 °C for 2 min to accelerate the saturation of water vapor in the vessel. Afterward, the chloroform solution of P6 was taken using a syringe, and the needle of the syringe penetrated the plastic wrap to cast the polymer solution onto the silicon wafer under humid condition. The pinhole on the plastic wrap was immediately pasted with transparent tape to keep the vessel sealed. Finally, the polymer-coated silicon wafer was taken out after the experimental device was placed at room temperature for another 30 min. The morphology of the obtained thin films of P6 on silicon wafers were characterized using SEM (Thermo APREO S) and an inverted fluorescence microscope (IX73) under the light irradiation with excitation wavelength of 400–440 nm.

### **Preparation of Polymer Nanoparticles (NPs):**

1 mL of the THF solution containing 1.0 mg polymer (P6 or *hb*-P3) and 2.0 mg DSPE-PEG<sub>2000</sub> was slowly added into 10 mL distilled water under sonication by a microtip probe sonicator (XL2000, Misonix Incorporated, NY) with 45% output for 2 min. The mixture was then transferred into a dialysis tube (MWCO 3500 Da) and dialyzed against deionized water for 24 h. In order to remove THF completely, the water was replaced by fresh water every 4 h. The final obtained nanoparticle solutions were concentrated by ultrafiltration before use.

### **Cell Culture and Cell Imaging:**

4T1 cells were cultured with RMPI-1640 medium containing 10% fetal bovine serum and 1% penicillin-streptomycin at 37 °C in a humidified environment of 5% CO<sub>2</sub>. For the cell imaging experiment, the harvested cells were seeded in a glass bottom dish at a suitable density and culture for 24 h. The cells were then incubated with fresh 1640 medium containing the of P6 NPs (20 µg/mL) or *hb*-P3 NPs (20 µg/mL) for 4 h, following incubated with LysoTracker Red (LTR) (1 µM) for 30 min and washed with PBS for twice. After that, cells were imaged by a confocal laser scanning microscope (CLSM, Zeiss-LSM 980). Excitation wavelength: 405 nm for polymers and 561 nm for LTR; emission filter: 420–650 nm for polymers and 650–700 nm for LTR.

### **Evaluation of Cytotoxicity and Photostability:**

The cytotoxicity of P6 and *hb*-P3 to 4T1 cells was measured by the traditional methylthiazolyldiphenyltetrazolium (MTT) assay according to the manufacturer's method (n = 6). For each cell line, the cells were seeded in 96-well plates at a density of  $6 \times 10^3$  cells/well. After culture for 24 h, the medium was replaced by fresh medium that contains different concentrations of polymer NPs. After further incubation for 24 h, the previous medium was removed and 100 µL of pure 1640 medium containing 10% MTT (5 mg/mL) was added into each well. The cells were further incubated at 37 °C for 3 h. Then the medium was carefully removed and 100 µL of DMSO was added to dissolve the purple crystals. The absorption at 570 nm was then measured with a microplate reader (BioTek). The

cell viability was expressed by the ratio of the absorbance of the cells incubated with various polymer concentrations to that of cells incubated with the culture medium only. Each of the experiments was performed at least three times.

The photostability of **P6** and *hb*-**P3** was demonstrated from the fluorescence images of 4T1 cells stained with polymer NPs (20 µg/mL, 4 h) collected under the continuous light irradiation with 405 nm laser for 60 loops. The obtained fluorescence images were then statistically analyzed using image processing software. To quantify the change in the fluorescence intensity of the polymers, the fluorescence signal of the image at the first loop was defined as the original fluorescence intensity.



**Scheme S1.** Possible mechanism for the formation of 2,5-disubstituted 1,3,4-oxadiazole derivatives.

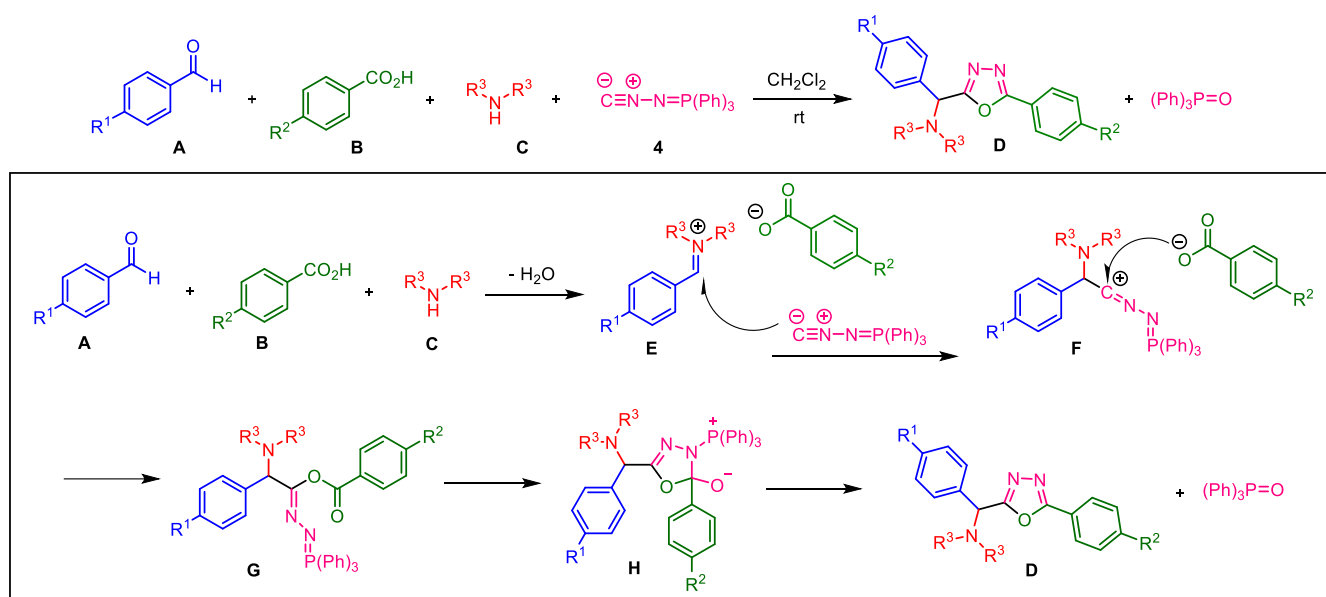


**Table S1.** Optimization of the polymerization conditions for the synthesis of hyperbranched polymers.<sup>a</sup>

entry	polymer	[1] (M) <sup>b</sup>	[1]/[2]/[3]/[4]	time (h)	atmosphere	yield (%)	$M_n$ (MALLS) <sup>c</sup>	$M_w$ (MALLS) <sup>c</sup>	$\bar{D}$
1	hb-P1	0.10	1.0/1.0/2.4/2.4	24	$\text{N}_2$	50	6300 <sup>d</sup>	9100 <sup>d</sup>	1.4 <sup>d</sup>
2	hb-P2	0.10	1.0/1.0/2.4/2.4	24	$\text{N}_2$	50	7600 <sup>d</sup>	10300 <sup>d</sup>	1.3 <sup>d</sup>
3	hb-P1	0.18	1.0/1.0/2.0/2.0	24	air	66	66400	124100	1.9
4	hb-P1	0.18	1.0/1.0/2.0/2.0	3	air	55	4300	5000	1.2
5	hb-P2	0.18	1.0/1.0/2.0/2.0	3	air	73	6700	8100	1.2
6	hb-P3	0.10	1.0/1.0/2.4/2.4	24	$\text{N}_2$	49	8100 <sup>d</sup>	12200 <sup>d</sup>	1.5 <sup>d</sup>
7	hb-P3	0.18	1.0/1.0/2.0/2.0	3	air	45	46300	64500	1.4

<sup>a</sup> Unless otherwise noted, the polymerizations were carried out at room temperature. <sup>b</sup> Monomer concentration was calculated considering the volume of both the solvent and the amine liquid. <sup>c</sup> Absolute molecular weights were determined by GPC using a multiangle laser light scattering (MALLS) detector in THF. Dispersity ( $\bar{D}$ ) =  $M_w/M_n$ . <sup>d</sup> The samples are partially soluble and the GPC data are for the soluble fraction.

**Scheme S2.** Synthetic route to model compound **5**.

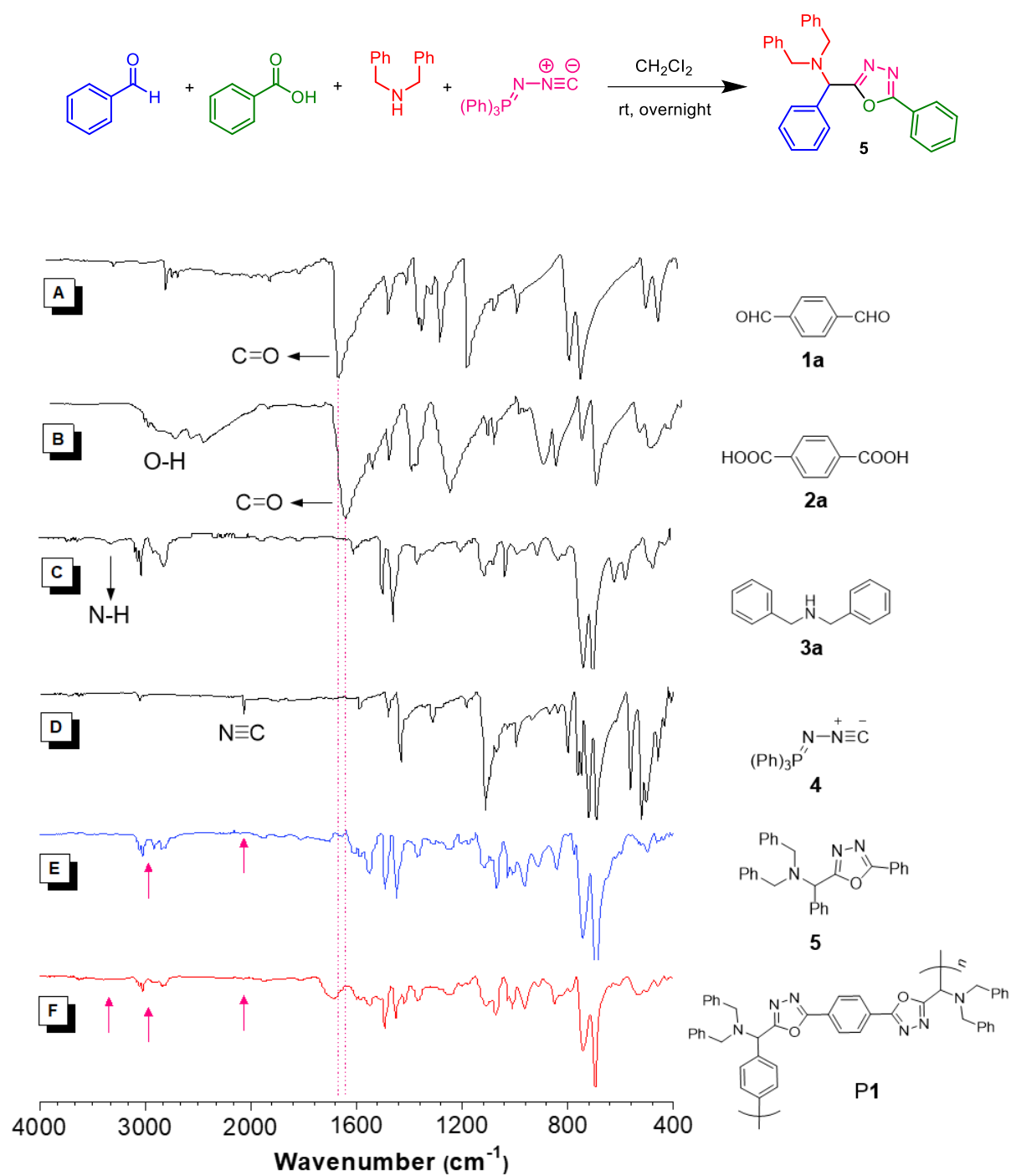


**Figure S1.** IR spectra of (A) **1a**, (B) **2a**, (C) **3a**, (D) **4**, (E) model compound **5**, and (F) **P1**.

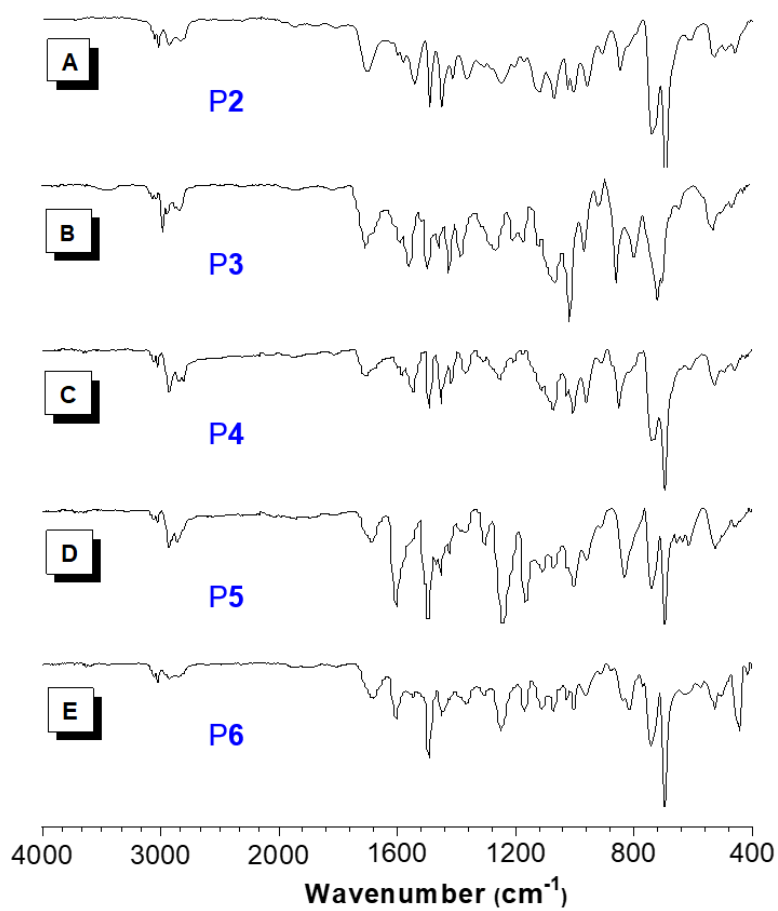


**Figure S2.** IR spectra of (A) P2, (B) P3, (C) P4, (D) P5, and (E) P6.

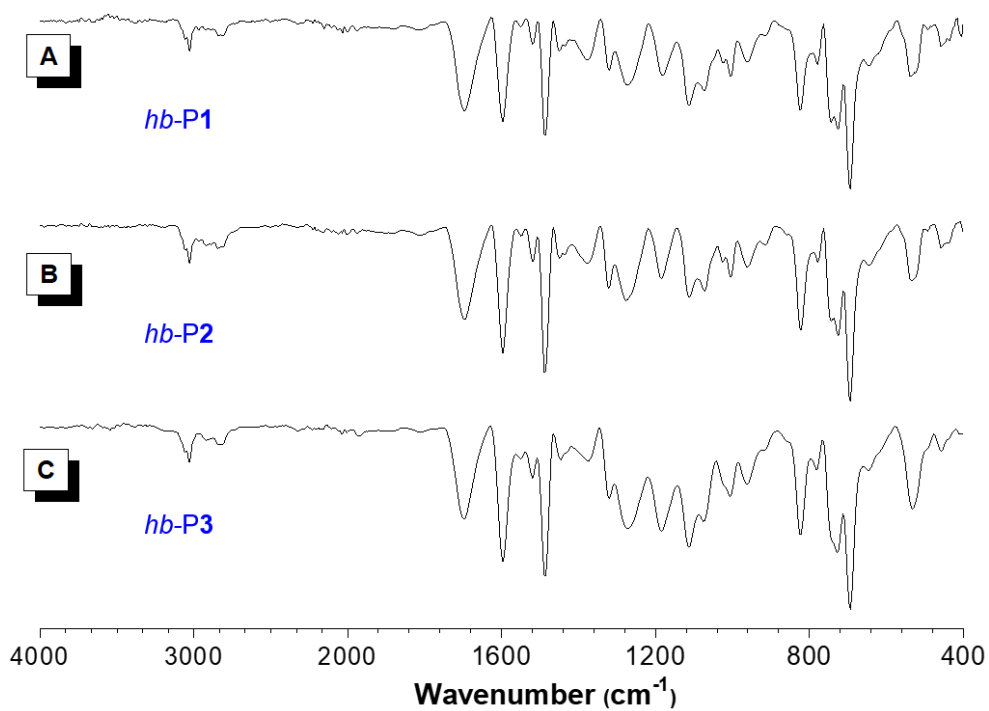


**Figure S3.** IR spectra of (A) *hb*-P1, (B) *hb*-P2, and (C) *hb*-P3.

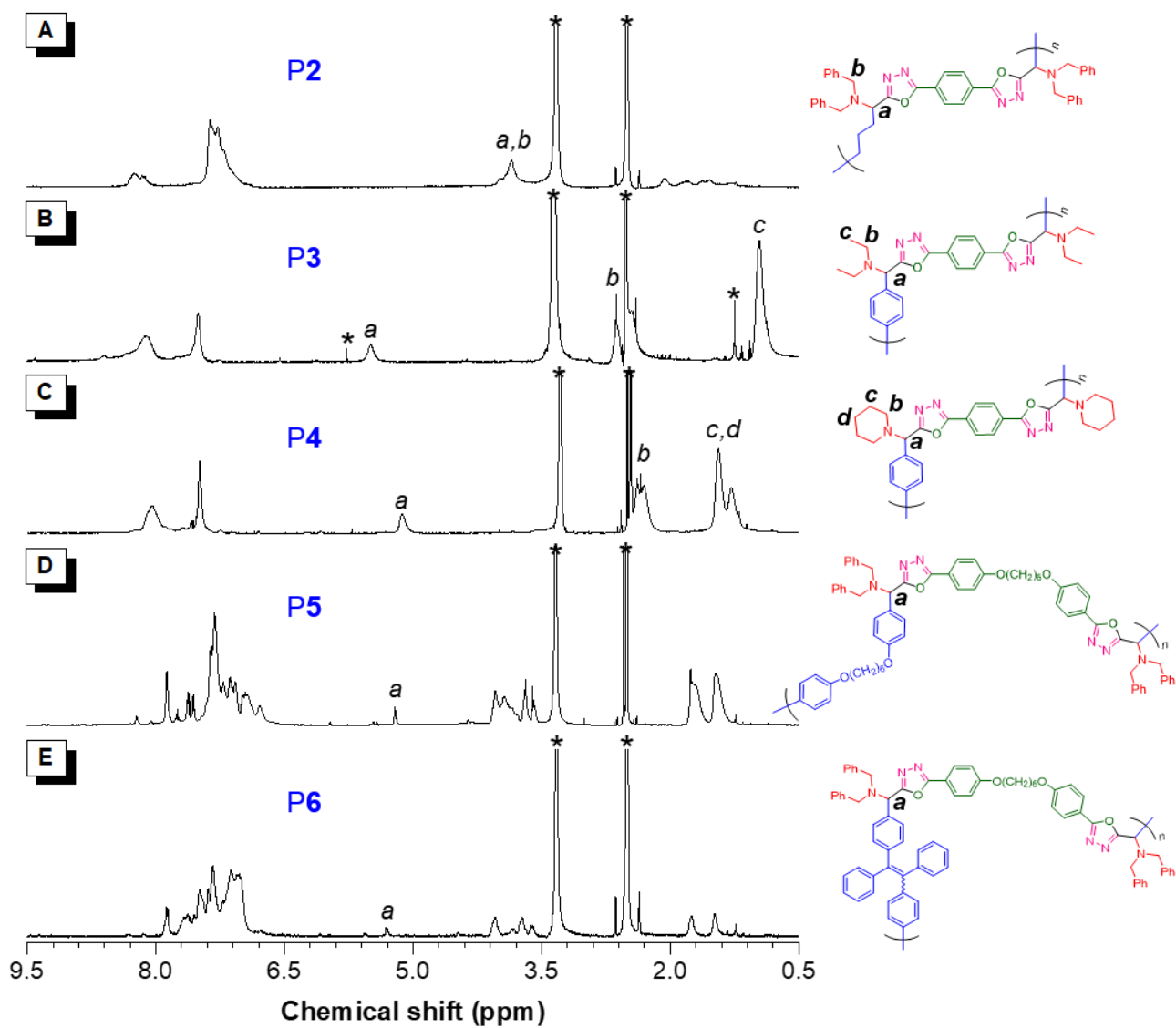


**Figure S4.**  $^1\text{H}$  NMR spectra of (A) P2, (B) P3, (C) P4, (D) P5, and (E) P6 in  $\text{DMSO-}d_6$ .

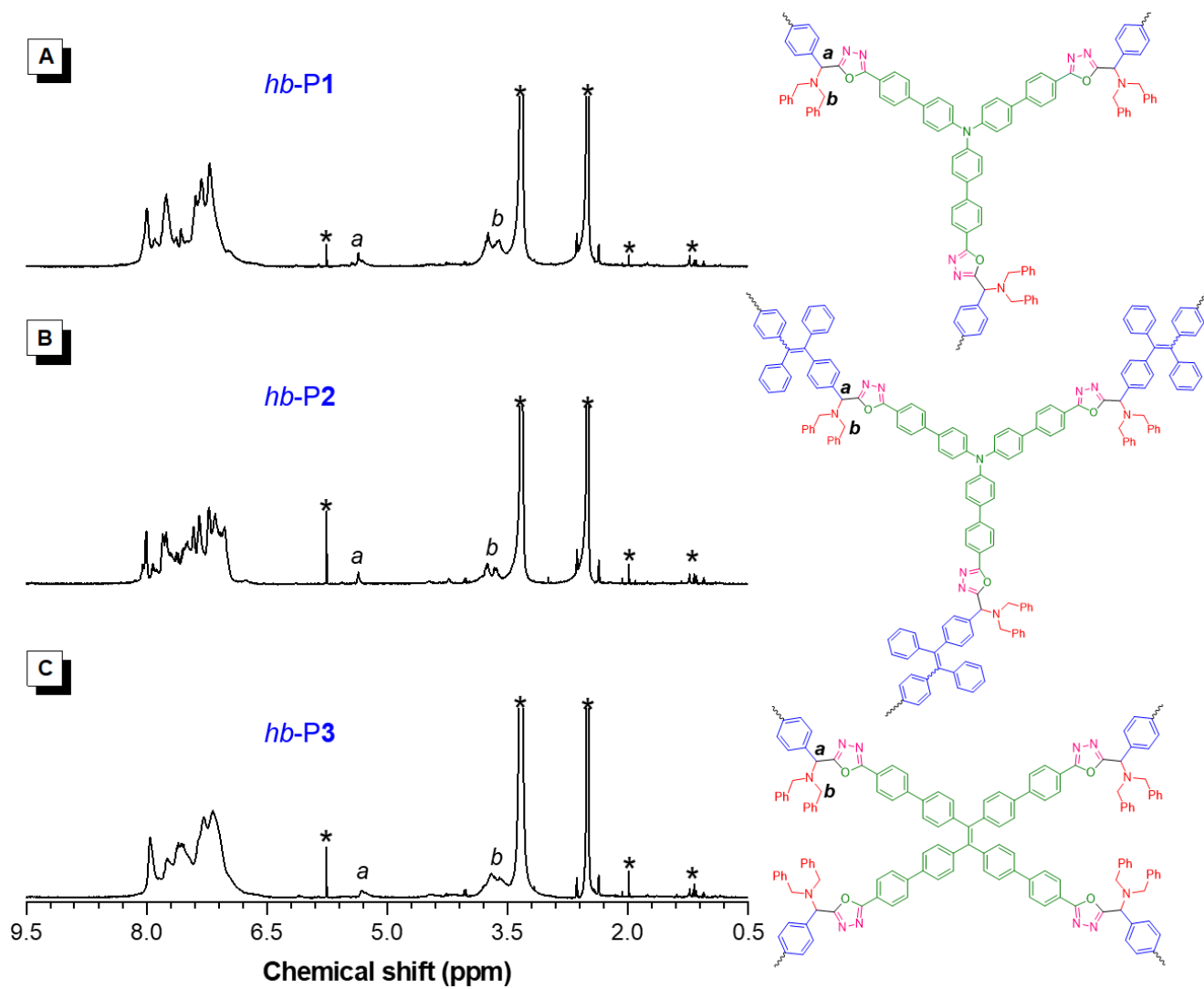


**Figure S5.**  $^1\text{H}$  NMR spectra of (A) *hb-P1*, (B) *hb-P2*, and (C) *hb-P3* in  $\text{DMSO-}d_6$ .

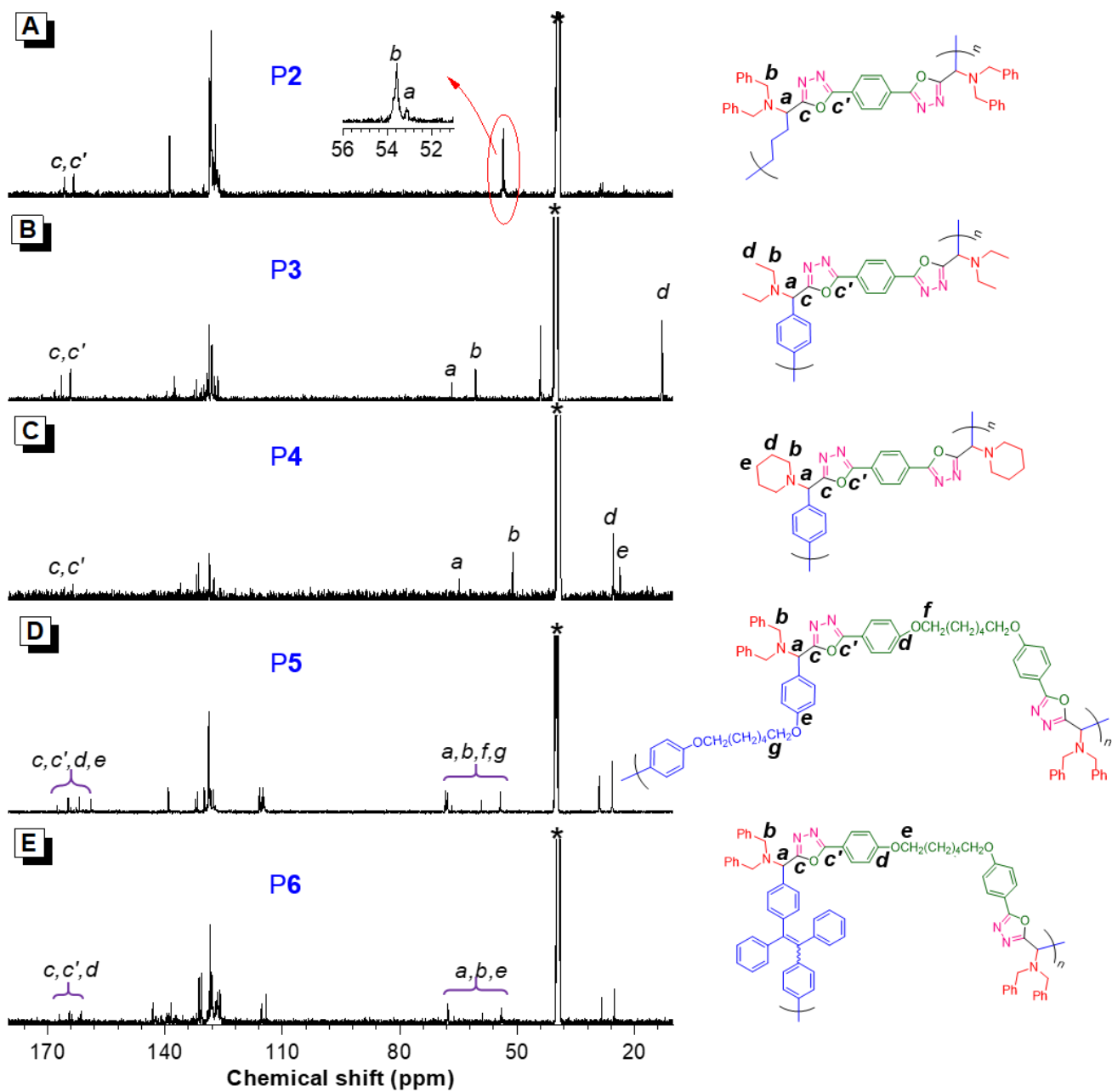


**Figure S6.**  $^{13}\text{C}$  NMR spectra of (A) P2, (B) P3, (C) P4, (D) P5, and (E) P6 in  $\text{DMSO-}d_6$ .

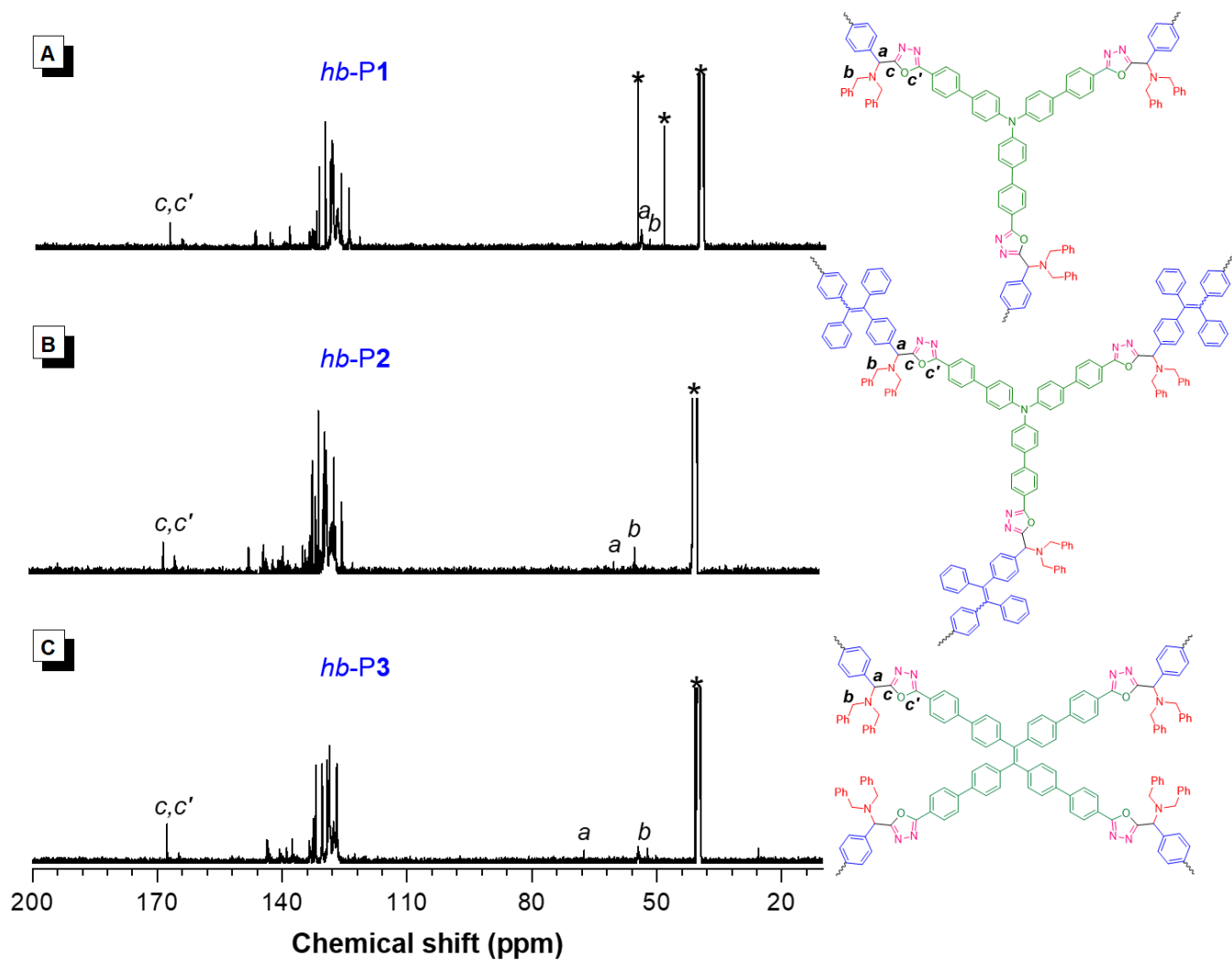


**Figure S7.**  $^{13}\text{C}$  NMR spectra of (A) *hb-P1*, (B) *hb-P2*, and (C) *hb-P3* in  $\text{DMSO-}d_6$ .

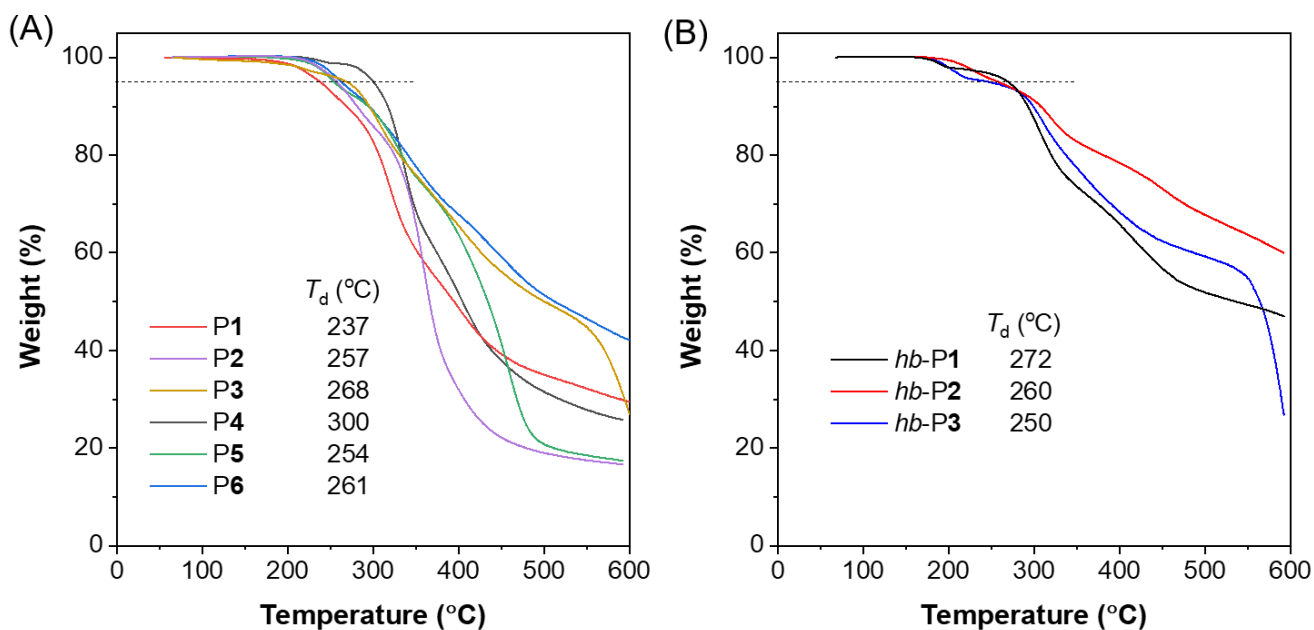


**Figure S8.** TGA thermograms of (A) linear polymers P1–P6 and (B) hyperbranched polymers *hb*-P1–*hb*-P3 recorded under nitrogen at a heating rate of 10 °C/min.

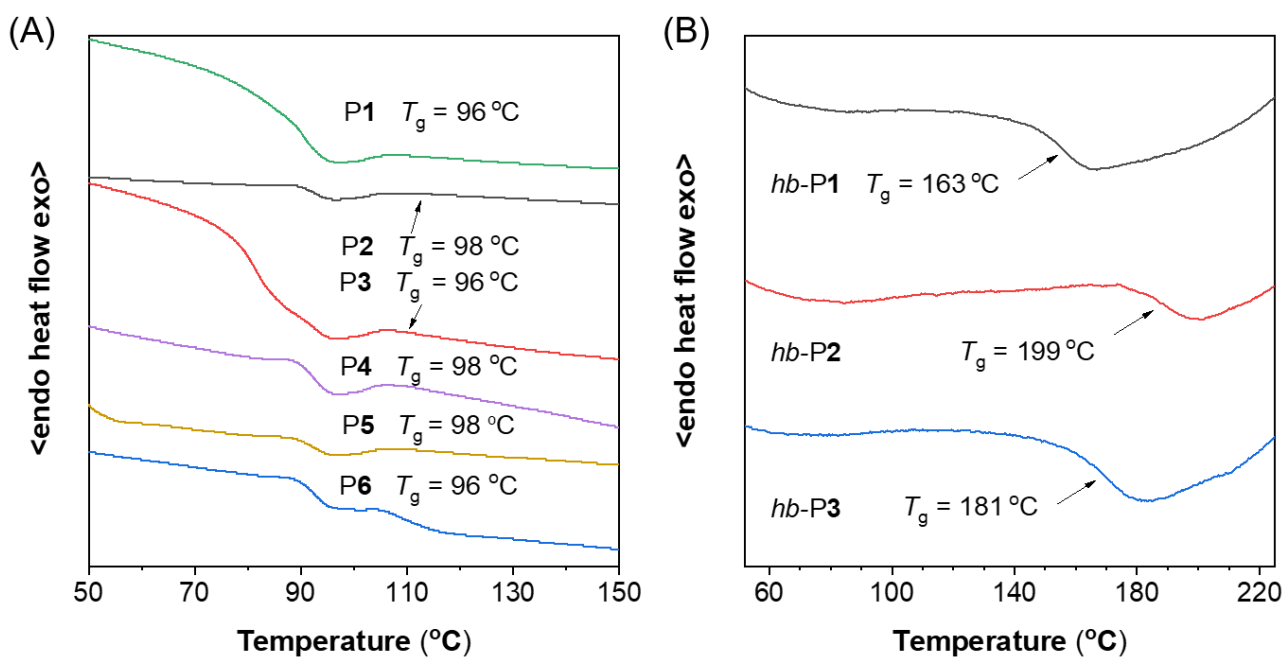


**Figure S9.** DSC thermograms of (A) P1–P6 and (B) *hb*-P1–*hb*-P3 recorded under nitrogen during the second heating cycle at a heating rate of 10 °C/min.



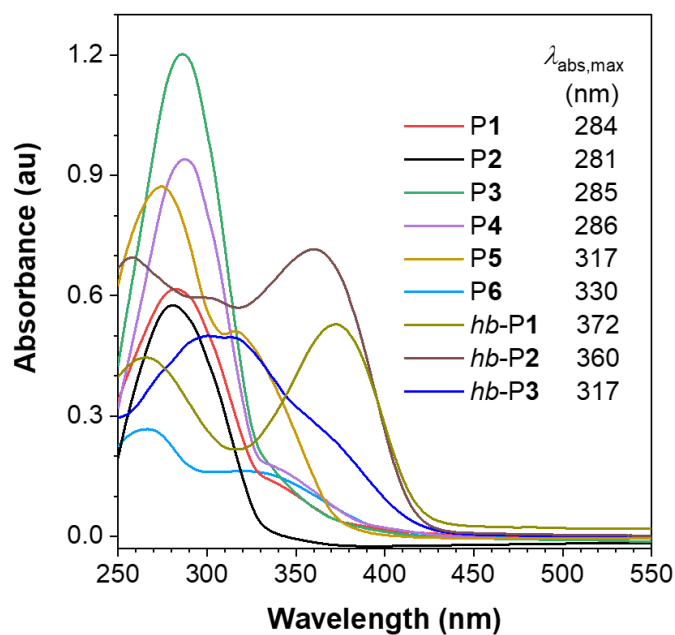


**Figure S10.** UV-vis absorption spectra and the maximum absorption wavelengths of P1–P6 and *hb*-P1–*hb*-P3 in their THF solutions. Solution concentration: 10  $\mu$ M.

**Table S2.** Fluorescence quantum yields of polymers in different states.

polymer	$\Phi_{\text{soln}}$	$\Phi_{\text{aggr}}$	$\Phi_{\text{film}}$
P6	0.6%	4.5% ( $f_w = 80\%$ )	1.2%
		2.6% ( $f_w = 90\%$ )	
<i>hb</i> -P3	3.9%	14.1% ( $f_w = 70\%$ )	6.4%
		6.6% ( $f_w = 90\%$ )	
<i>hb</i> -P1	31.6%	4.5% ( $f_w = 90\%$ )	11.9%
<i>hb</i> -P2	26.8%	4.5% ( $f_w = 90\%$ )	4.3%

<sup>a</sup> Abbreviation:  $\Phi_{\text{soln}}$ ,  $\Phi_{\text{aggr}}$ ,  $\Phi_{\text{film}}$  = the fluorescence quantum yield of the THF solution, aggregates in THF/water mixtures with different water fractions ( $f_w$ ), and the solid film of polymers, respectively.

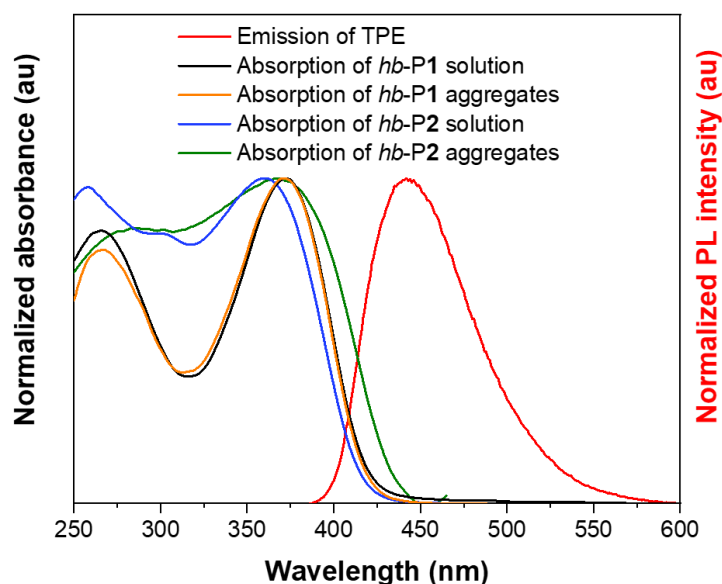


**Figure S11.** Normalized UV-vis absorption spectra of *hb-P1* and *hb-P2* in different states and the normalized PL spectrum of TPE in THF solution. Solution concentration: 10  $\mu\text{M}$ . The absorption spectra of *hb-P1* and *hb-P2* aggregates were measured on their THF/water suspension with a water fraction of 90%.

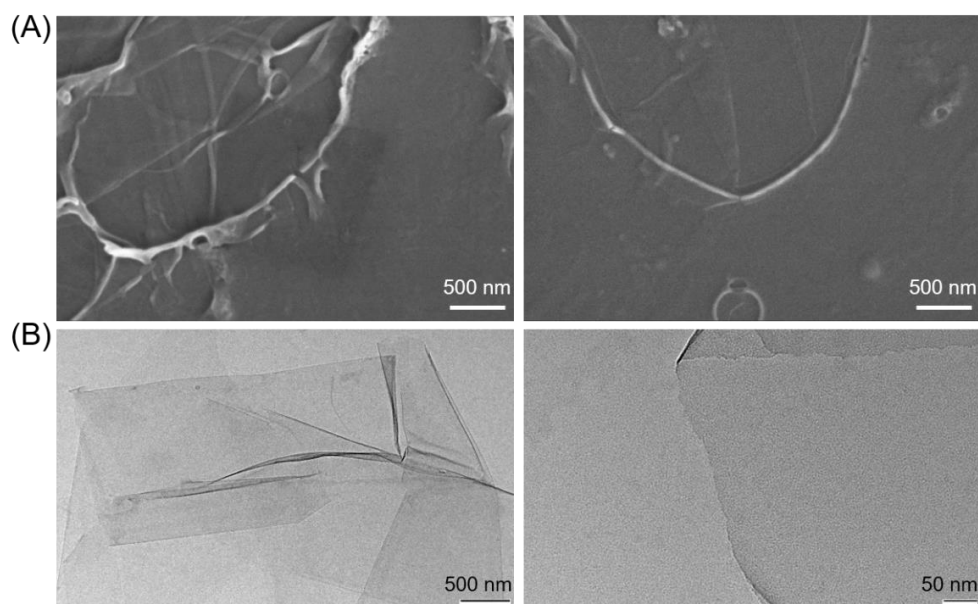


**Figure S12.** (A) SEM and (B) TEM images of the thin films prepared by the solvent evaporation of the chloroform solution of polymer **P3** on the surface of a silicon wafer or TEM support grids. Solution concentration: 0.01 mg/mL.



**Figure S13.** Fluorescence image showing the morphology of the thin film obtained by the solvent evaporation of the chloroform solution of P6 on a silicon wafer. Solution concentration: 0.1 mg/mL.

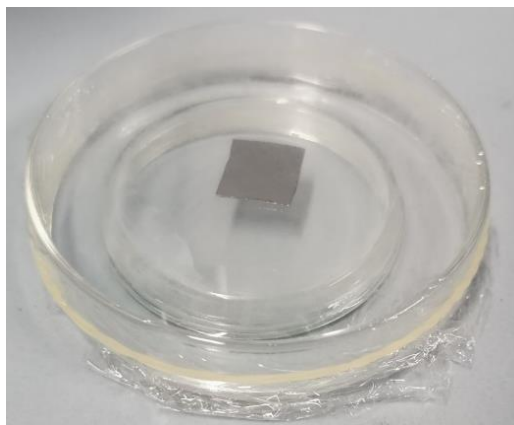


**Figure S14.** Experimental set-up for the fabrication of porous thin films of P6 using the breath figure method.

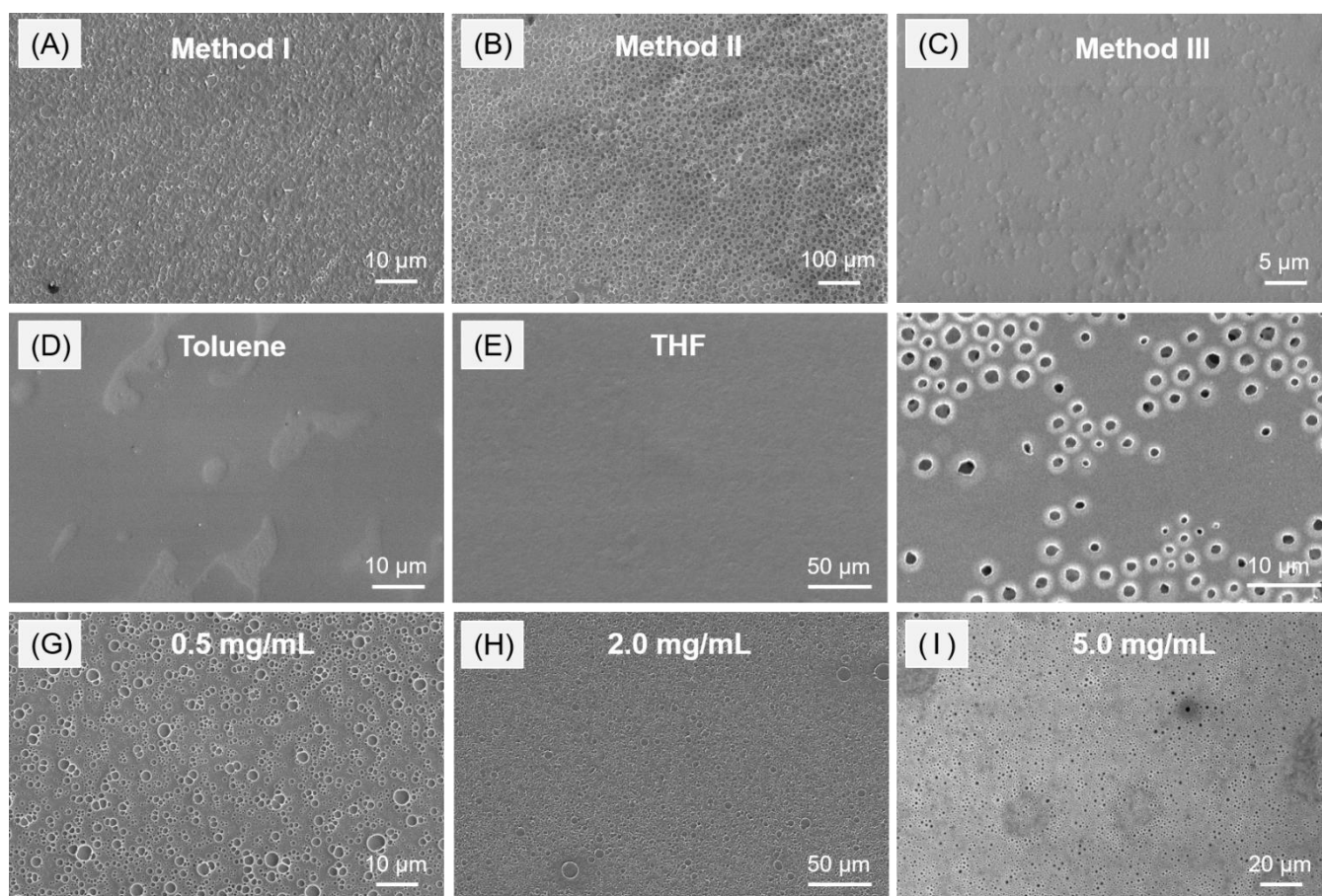


**Figure S15.** (A–C) SEM images of the film morphology formed by the chloroform solution of P6 (1.0 mg/mL) using different methods of establishing humid environment. (D–F) SEM images showing the influence of organic solvents on the film morphology of P6. Solution concentration: 1.0 mg/mL. (G–I) SEM images showing the influence of the concentration of the chloroform solution of P6 on the film morphology.

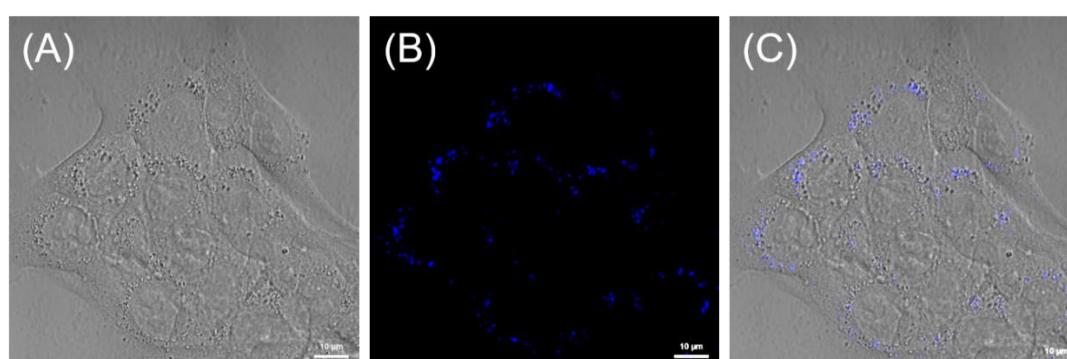


**Figure S16.** (A) The bright-field image, (B) fluorescence image, and (C) the merged image of the fluorescence images and the bright-field image of 4T1 cells stained with P6 (10 μg/mL, 2 h). Scale bar = 10 μm. Excitation wavelength: 405 nm; emission filter: 420–650 nm.

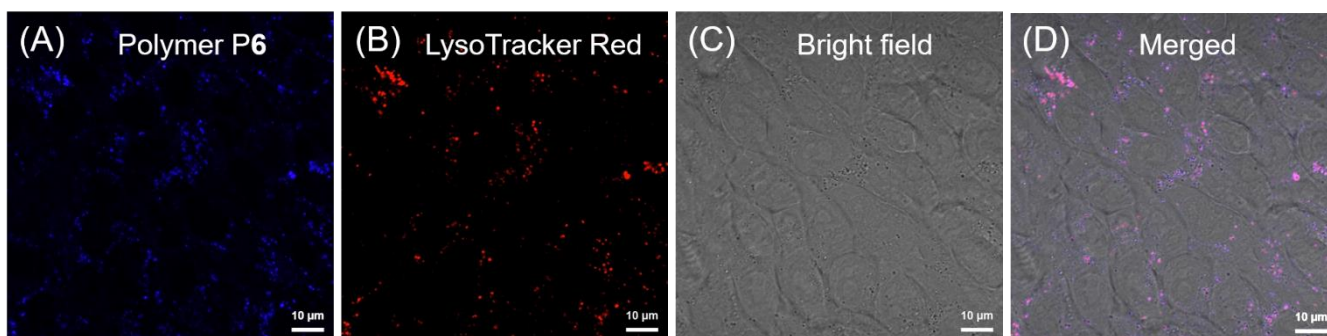


**Figure S17.** (A and B) Confocal images of 4T1 cells stained with (A) P6 (20 µg/mL, 4 h, DMSO stock solution) and (B) LysoTracker Red (LTR, 1 µM, 30 min). (C) The associated bright-field image. (D) The merged image of the fluorescence images and the bright-field image. Scale bar = 10 µm. Excitation wavelength: 405 nm for polymers and 561 nm for LTR; emission filter: 420–650 nm for polymers and 650–700 nm for LTR.

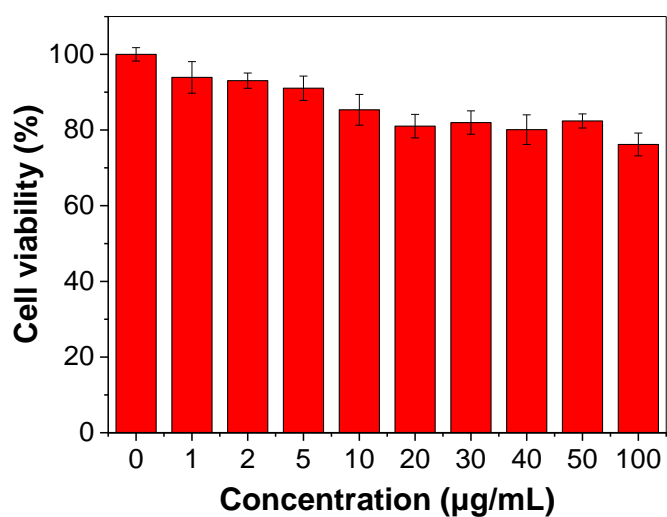


**Figure S18.** Cell viability of 4T1 cells in the presence of P6 (DMSO stock solution) at different concentrations.

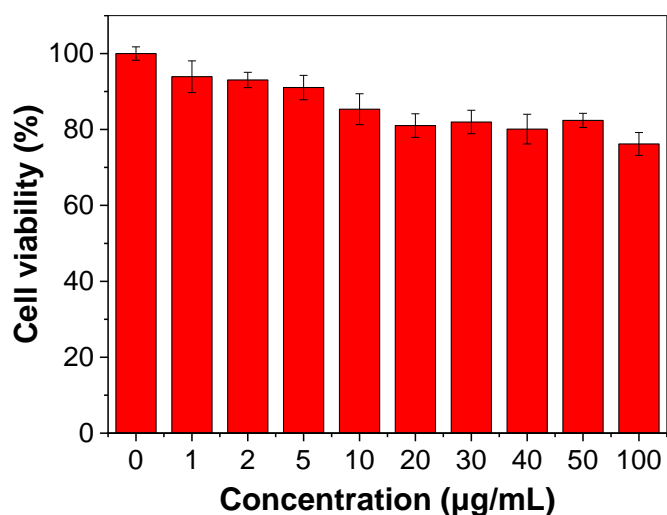


**Figure S19.** Cell viability of 4T1 cells in the presence of *hb-P3* (DMSO stock solution) at different concentrations.

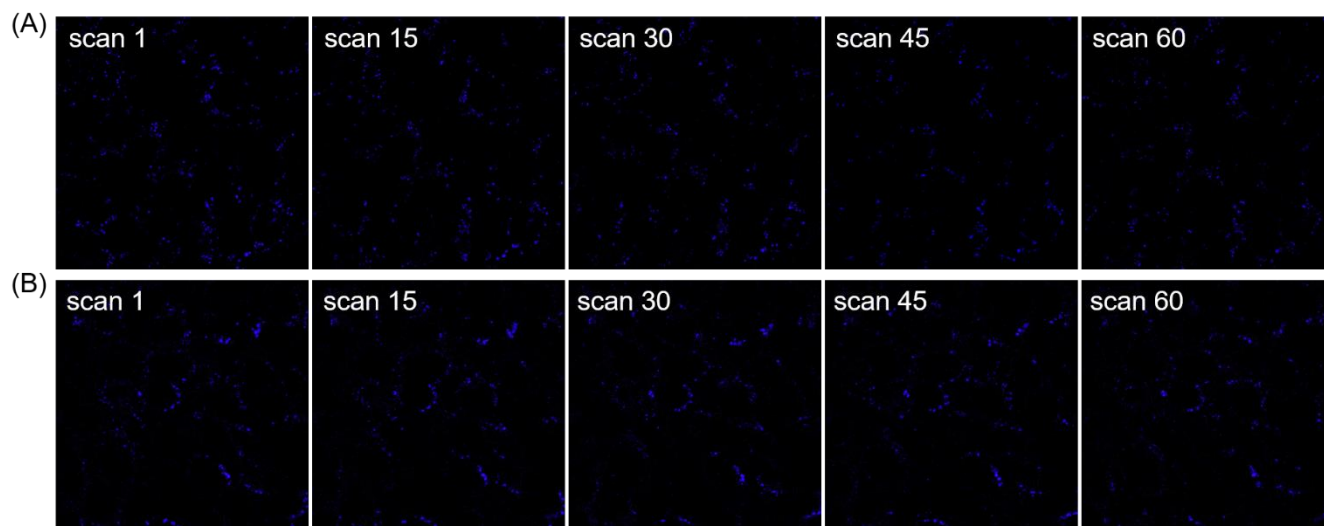


**Figure S20.** Fluorescence images of 4T1 cells obtained at different scan time. The 4T1 cells were stained with (A) P6 nanoparticles (20 µg/mL, 4 h) and (B) *hb-P3* nanoparticles (20 µg/mL, 4 h).

## References

- [1] a) Abdelfattah, A. M.; Mekky, A. E. M.; Sanad, S. M. H. *Synth Commun* **2022**, 52, 1421-1440; b) Karabulut, A.; Lafzi, F.; Bayindir, S.; Sevgili, Ö.; Orak, I. *J. Mol. Struct.* **2021**, 1231, 129699; c) Naranjo, C.; Dorca, Y.; Ghosh, G.; Gómez, R.; Fernández, G.; Sánchez, L. *Chem Comm* **2021**, 57, 4500-4503; d) Qiao, G.-Y.; Yuan, S.; Pang, J.; Rao, H.; Lollar, C. T.; Dang, D.; Qin, J.-S.; Zhou, H.-C.; Yu, J. *Angew. Chem. Int. Ed.* **2020**, 59, 18224-18228.
- [2] Ramazani, A.; Rezaei, A. *Org. Lett.* **2010**, 12, 2852-2855.